Published in final edited form as:
Neuroimage. 2012 January 16; 59(2): 1912–1923. doi:10.1016/j.neuroimage.2011.08.102.

Impact of state anxiety on the interaction between threat monitoring and cognition

Jong Moon Choi, **Srikanth Padmala**, and **Luiz Pessoa**
Department of Psychology, University of Maryland, College Park, MD, USA

Abstract

How does threat processing impact cognitive performance? To investigate this question, in the present functional magnetic resonance imaging study, participants performed a response-conflict task (neutral, congruent, and incongruent trials) that followed a variable-length shock anticipation period or a corresponding delay during which they would not be shocked. The delay period was cued by a geometric-shaped stimulus indicating whether the subject was in the safe (no shock) or threat (potential shock) condition. Behaviorally, participants showed increased reaction time interference (incongruent – neutral) during threat trials, an effect that increased as a function of state anxiety level across participants. Brain imaging data were analyzed for the cue and the subsequent target phase of the task. At the target phase, the left anterior insula exhibited interaction-type responses (i.e., increased interference during threat trials) that were positively associated with state anxiety level – a relationship that paralleled the behavioral pattern. At the cue phase, greater responses to threat vs. safe were observed in a circuit of regions, including the medial PFC, anterior insula, thalamus, and bed nucleus of the stria terminalis/caudate, which we interpreted as engaged by shock monitoring/anticipation processes. In contrast, intriguingly, greater responses to safe vs. threat at the cue phase were observed in a broader set of regions that overlapped with the “resting-state” network. Finally, a standard statistical mediation analysis revealed that the relationship between state anxiety scores and interference-related responses in the left anterior insula during the target phase was partially mediated via cue responses in the medial PFC, consistent with the idea that more anxious individuals had difficulty in engaging the medial PFC during the threat condition. Taken together, our findings suggest that threat monitoring impairs the upcoming resolution of interference. Furthermore, a confluence of effects of cognitive task condition, threat, and individual differences in state anxiety was observed in the anterior insula, a structure that is suggested to be particularly important for the interaction between emotion and cognition.

Keywords

threat; cognition; anxiety; response conflict; emotion

Corresponding author: Luiz Pessoa, Department of Psychology, University of Maryland, College Park, MD 20742, pessoa@umd.edu, Phone: 301-405-2423.

Introduction

In the past decade, a growing body of studies has investigated the impact of emotional stimuli on cognitive function. For instance, in a working memory task, negative distractors impair behavioral performance to a larger extent than neutral items (Dolcos and McCarthy, 2006; Anticevic et al., 2010). The impact of emotion on many other cognitive tasks has been investigated, including conflict processing (Blair et al., 2007; Hart et al., 2010; Kanske and Kotz, 2010) and response inhibition (Pessoa et al., 2011). This literature has focused on paradigms in which the role of emotion is closely associated with a stimulus (typically an unpleasant picture). Another central property of these paradigms is that the temporal characteristics of the emotional stimulus are generally known to the participants and fixed.

At the same time, recent studies have attempted to understand the impact of more temporally extended emotional manipulations, so as to approximate conditions that are closer to anxiety than fear (Davis et al., 2010). Along these lines, in the present study, our goal was to investigate cognitive performance subsequent to a period of shock anticipation. Participants performed a cognitive task during two experimental contexts (Fig. 1). An initial cue stimulus signaled whether the trial was “safe” or “threat”. During threat trials, mild electric shock was administered to participants in a third of the trials during a variable-length delay period in a way that the timing of the shock was unpredictable to participants. During safe trials, the trial timing and structure were the same, except that no shocks were administered. Following the anticipation period, participants were asked to determine if a picture contained a house or building while ignoring task-irrelevant words, which were used to create neutral, congruent, and incongruent trials – we refer to this latter task period as the “target” phase.

We hypothesized that monitoring for a potential shock affects task performance via its impact on capacity-limited information processing –much like strong emotional stimuli, as suggested in the dual competition framework (Pessoa, 2009). Accordingly, shock monitoring would use processing resources needed for subsequent conflict processing, thereby having its largest impact on incongruent trials, during which response conflict must be adequately resolved to ensure correct task behavior.

As shown in Figure 1, the task was designed such that the cue and target phases were separated by a short, variable-length duration period. Whereas one goal of this manipulation was to generate temporal uncertainty regarding potential shock delivery, a second goal was to allow us to independently estimate evoked responses to both task phases. Regarding the former, this allowed us to contrast responses evoked by the cue during trials that were structurally identical, except for the geometric shape of the cue stimulus (trials that actually contained a physical shock were discarded from the main analyses). Previous studies have identified a number of regions involved in threat monitoring, including dorsomedial prefrontal cortex (PFC), anterior insula, bed nucleus of the stria terminalis (BNST), and thalamus, among others (Kalin et al., 2005; Chandrasekhar et al., 2008; Mobbs et al., 2010; Somerville et al., 2010). The BNST is especially interesting given its potential involvement in monitoring escalating threat levels (see Davis et al., 2010 for a review). The anterior insula is also particularly relevant because it is critically involved in the processing of bodily signals and contains a visceral sensory cortex that maps the internal state of the body in a precise fashion (Craig, 2002, 2009). Accordingly, we anticipated that, in our task, threat as signaled by the cue stimulus would engage some of these regions.

A central goal of our study was to understand the impact of threat monitoring on responses evoked during task execution, which was possible, again, given that our design allowed separate estimation of target phase responses. The medial PFC has been suggested to have

an important role in conflict processing and other effortful functions (Botvinick et al., 2001; Brown and Braver, 2005; Weissman et al., 2005). In a recent study, conflict-related responses in medial PFC *decreased* during trials in which participants could earn a reward for fast and accurate performance (Padmala and Pessoa, 2011). In the present experiment, instead, we expected that conflict-related responses in medial PFC would *increase* during the threat condition (vs. safe) – because threat was expected to increase response interference. A region of particular interest during the target phase was, again, the anterior insula, which not only is strongly implicated in emotional processing, but also during cognitive function. Indeed, the anterior insula is consistently engaged during a range of cognitive tasks (Dosenbach et al., 2006; Van Snellenberg and Wager, 2009). Given that both shock monitoring and response conflict were involved in our task, the anterior insula might constitute a site where emotional and cognitive information interact.

Finally, we were interested in understanding how individual differences influenced both behavioral performance and brain responses. Behaviorally, we anticipated that greater response interference would be observed in participants with higher state and/or trait anxiety. Brain responses were also anticipated to vary based on individual differences during the cue and target phases of the task. In particular, the medial PFC and thalamus are involved in the regulation of anxiety-related behaviors in non-human primates (e.g., Kalin et al., 2005). Human neuroimaging studies have described the engagement of the medial PFC during emotion regulation, too (Banks et al., 2007; for review Ochsner and Gross, 2005). If, during our task, these structures also performed regulatory functions, their recruitment during the cue phase could also vary as a function of state/trait anxiety. In particular, participants with higher levels of anxiety might exhibit *weaker* cue-related responses in these regions, possibly reflecting the participant's inability to adequately regulate their emotion. In addition, of particular interest was the possibility that cognitive-emotional interactions during the target phase depended on individual differences, too. In this scenario, the interaction between shock monitoring and response interference would be a function of state/trait anxiety levels – e.g., an emotion x cognition statistical interaction would be evident for high-but not low-anxious individuals.

Materials and Methods

Subjects

Forty-seven volunteers participated in the study, which was approved by the Institutional Review Board of Indiana University, Bloomington. Participants were screened during the recruitment process based on self-reports concerning the following items: not be taking psychoactive drugs (including Zoloft, Ritalin, and drugs of abuse); have no known psychological condition (including ADD, depression, PTSD, and clinical anxiety); have no known neurological condition (including stroke, seizure, brain tumor, or closed head injury). All participants were right-handed, had normal or corrected-to-normal vision, and gave informed written consent. One male participant's data were excluded from the analysis because of poor performance (no response on 29 % of trials); in addition, data from five male participants were removed because of excessive head motion (exceeding one voxel size). Thus, data from forty-one participants (21±2.40 years old; 22 females) were included in the final analysis.

Personality questionnaire

Prior to the experiment, participants completed the Spielberger State-Trait Anxiety Inventory (Spielberger, 1970). The trait portion of the inventory was completed one or two days prior to the fMRI session, and the state portion was completed immediately before scanning.

Stimuli and behavioral paradigm

Each trial started with the presentation of a rectangle- or diamond-shaped cue stimulus (750 ms) that indicated the anticipation condition (safe, threat), followed by a 1.75 – 5.75 s variable delay period. The threat cue, which was counterbalanced across participants, indicated that a mild electric shock could be delivered during the delay period. To calibrate the intensity of the electric shock, each participant was asked to choose his/her own stimulation level immediately prior to functional imaging, such that the stimulus would be "highly unpleasant but not painful". After each run, participants were asked about the unpleasantness of the stimulus and were asked to, if needed, re-calibrate it so that the shock would still be "highly unpleasant but not painful". Shocks were administered with an electrical stimulator (Coulbourn Instruments, PA, USA) on the fourth ("ring") and fifth ("pinky") fingers of the non-dominant left hand. During the threat condition, physical shocks were administered on 33% of the trials (participants were not informed about the probability of shock).

Following the delay, the target display was presented for 500 ms, followed by a 1.75 – 5.75 s variable inter-trial interval (ITI). For the target display, a picture of a house or building (4.1° × 4.1°) overlaid with a five-letter string (2.1° × 0.5°) was presented (Fig. 1). The strings employed were "HOUSE", "BLDNG", or "XXXXX", creating congruent, incongruent, or neutral trials. Stimuli were designed so as to capitalize on response properties of visual cortex. Specifically, scenes strongly recruit the bilateral parahippocampal gyri (Epstein et al., 1999), whereas words robustly engage the left fusiform gyrus (Polk and Farah, 2002; McCandliss et al., 2003). Participants were instructed to press the index-finger button for a building picture or the middle-finger button for a house picture regardless of the overlaid word (responses were always made with the right hand; the response button mapping was counterbalanced across participants). Both delay and ITI durations were selected from an exponential distribution favoring shorter intervals and helped in the robust estimation of separate cue- and target-related responses (see below).

For the presentation of visual stimuli and recording of participant's responses, Presentation software (Neurobehavioral Systems, Albany, CA, USA) was used. Behavioral responses were collected using an MRI-compatible response box. Skin conductance response (SCR) data were also collected using the MP-150 system (BIOPAC Systems, Inc., CA, USA) at a sampling rate of 250 Hz by using MRI-compatible electrodes attached to the index and middle fingers of the left hand.

Each participant performed 6 "runs" of the main task (7 runs for one participant). Each run consisted of 54 trials, resulting in a total of 324 trials and 54 trials per condition. All experimental conditions were intermixed randomly but with the constraint that each possible trial combination occurred an equal number of times in terms of the anticipation condition and both previous- and current-trial congruency type. To keep the trial types balanced after exclusion of the actual physical-shock trials (see *Behavioral data analysis* below), the subsequent trial type after the physical-shock trial always belonged to the safe condition. In other words, the trial sequence was designed so as to be balanced *after* the exclusion of trials containing shocks and the subsequent safe trial. Finally, each run started and ended with a 20-s fixation cross, which assisted in establishing a baseline level of activity.

Functional localizer

Following the main experimental runs, an additional functional localizer run was conducted in which participants performed a simple one-back working memory task. During the run, a series of novel words or scene pictures (house/building) was presented in an alternating blocked fashion and participants were instructed to make a response to repeating stimuli.

Five blocks were performed per condition. Each stimulus was displayed for 1000 ms and followed by a 250-ms blank screen. Blocks lasted 15 s and were separated by a 15-s rest block during which participants passively viewed a white fixation cross on the screen.

MR data acquisition

MR data were collected using a 3 Tesla Siemens TRIO scanner (Siemens Medical Systems, Erlangen, Germany) with a 32-channel head coil (without parallel imaging). Each scanning session began with a high-resolution MPRAGE anatomical scan (TR = 1900 ms, TE = 4.15 ms, TI = 1100 ms, 1 mm isotropic voxels, 256 mm field of view). Subsequently, in each functional run of the main experiment, 169 EPI volumes were acquired with a TR of 2500 and TE of 25 ms. Each volume consisted of 44 oblique slices with a thickness of 3 mm and an in-plane resolution of 3 × 3 mm (192 mm field of view). Slices were positioned approximately 30 degrees relative to the plane defined by the line connecting the anterior and posterior commissures, a prescription that improves the quality of signals in the amygdala – for instance, using similar parameters, we were able to investigate links between trial-by-trial responses in the amygdala and visual awareness during the attentional blink (Lim et al., 2009). For the final functional localizer run, 123 EPI volumes were collected with the same scanning parameters.

Behavioral data analysis

Trials during which actual shocks were delivered and the subsequent (safe) trials were discarded, thus leaving 36 trials per trial type. Trials with response time (RT) exceeding three standard deviations from the condition-specific mean (1.15 %) were discarded from further analysis. For RT analysis, error trials were discarded, too. For each participant, mean RT and error rate data were determined as a function of *Monitoring* (safe, threat) and *Congruency* (neutral, congruent, incongruent). Analyses of variance (ANOVAs) were conducted on the mean RT and error data, with those variables as within-subject factors. The alpha-level adopted was .05.

Skin conductance responses (SCRs)

Three participant's SCR data were not collected due to technical problems (thus, 38 participant's data were analyzed). Each participant's SCR data were initially smoothed with a median-filter over 50 samples (200 ms) to reduce scanner-induced noise and resampled at 1 Hz. The pre-processed SCR data were analyzed using multiple linear regression by using the AFNI software package (Cox, 1996; http://afni.nimh.nih.gov/afni) in the same way as fMRI data; for related approaches, please see Bach, Flandin, Frinston, and Dolan (2009). The goal of the analysis was to estimate responses to safe and threat cue stimuli. Trials that involved physical shock, subsequent safe trials, as well as error and RT outlier trials were modeled using three additional regressors of no interest. No assumptions were made about the shape of the SCR function. Average response to each trial type was estimated via deconvolution. Responses were estimated starting from event onset to 15 s post onset using cubic spline basis functions (see fMRI analysis below for further discussion). Constant, linear, and quadratic terms were included for each run separately (as covariates of no interest) to model baseline and drifts of the SCR. As an index of response strength, for each event type, we used the peak estimated response between 1–6 s after stimulus onset (as determined via the spline-based estimates). In order to equalize variance, response-strength indices were transformed by using a logarithm function [$\log_{10}(1+\text{SCR})$]. Of note, the general results estimated by the deconvolution procedure did not deviate from results calculated by subtracting a baseline (average signal between 0 and 1 s) from the peak amplitude during the 1–6 s time window following cue onset (Prokasy and Raskin, 1974).

General fMRI data analysis

Pre-processing of the data was done using tools from the AFNI software package (Cox, 1996; http://afni.nimh.nih.gov/afni). The first 3 volumes of each functional run were discarded to account for equilibration effects. The remaining volumes were slice-time corrected using Fourier interpolation such that all slices were realigned to the first slice to account for the timing offset between slices. Six-parameter rigid-body motion correction within and across runs was performed using Fourier interpolation (Cox and Jesmanowicz, 1999) such that all volumes were spatially registered to the first volume. To normalize the functional data to Talairach space (Talairach and Tournoux, 1988), initially each subject's high-resolution MRPAGE anatomical volume was spatially registered to the so-called TT_N27 template (in Talairach space) using a 12-parameter affine transformation; the same transformation was then applied to the functional data. All volumes were spatially smoothed using a Gaussian filter with a full-width at half maximum of 6 mm (i.e., two times the voxel dimension). Finally, the signal intensity of each voxel was scaled to a mean of 100.

Voxelwise analysis

Each participant's fMRI data were analyzed using multiple linear regression with AFNI. There were a total of 8 main event types in the design matrix: safe and threat events during the cue phase, and neutral, congruent, and incongruent events during the target phase, separately for the safe and threat conditions. Threat trials that involved physical shock, subsequent safe trials, as well as error and RT outlier trials were modeled separately using additional regressors of no interest (separately for the cue and target phases); note that even with trial removal, 32–34 trials were used on average for each of the experimental conditions, thus ensuring adequate representation. Constant, linear, and quadratic terms were included for each run separately (as covariates of no interest) to model baseline and drifts of the MR signal. As hemodynamic responses may have varied considerably across regions during the anticipation of shock (delay period), for the cue phase data, no assumptions were made about response shape. Cue-related responses were estimated starting from event onset to 15 s post onset using cubic spline basis functions. This method is closely related to the use of finite impulses ("stick functions"), the commonly employed technique that can be considered the simplest form of basis set. Cubic splines allow for a smoother approximation of the underlying responses, instead of the discrete approximation obtained by finite impulses. As an index of cue activation, we averaged the estimated responses at 5 and 7.5 s after stimulus onset (as determined via the spline-based estimates) for the safe and threat conditions, separately. For the target phase data, because responses were expected to be transient and essentially canonical, all regressors were convolved with a standard hemodynamic response function (Cohen, 1997). Accordingly, response strength was indexed in the standard way (i.e., by estimating a single regression coefficient per condition). Finally, data from all runs were concatenated and a single design matrix employed.

Event-related designs allow the estimation of different event types when they occur in a randomized fashion. However, the present study, by design, required a fixed order between the cue and target phases. In comparable situations, at times, a partial-trial design is employed (Ollinger et al., 2001). Because of several problems associated with this type of design (Ruge et al., 2009), here, instead, we randomized the delay between cue and target phases as well as the inter-trial interval (for a similar strategy, see Padmala and Pessoa, 2011). In this manner, correlations between different regressors were modest (they did not exceed .34), allowing us to separately estimate cue and target phase responses. Note that because the cue was always followed by the delay period, no attempt was made to separate cue responses from those during the delay period. Thus, although we refer to the responses

estimated with respect to cue onset as "cue related", they likely combined these two components.

Group analysis

Whole-brain voxelwise random-effects analyses were conducted separately for the cue and target phases and were restricted to grey-matter voxels based on the FSL automated segmentation tool (http://www.fmrib.ox.ac.uk/fsl/). For the cue phase, a paired *t* test was run to compare the activations between safe and threat conditions. For the target phase, a 2 × 2 repeated-measures ANOVA was run to investigate *Monitoring* (safe, threat), *Interference* (neutral, incongruent), and interaction effects (see Results for further elaboration). The alpha-level for voxelwise statistical analysis was determined by Monte-Carlo simulations using the 3dClustSim program of the AFNI toolkit (cluster-level alpha = .05; cluster extent: 19 voxels; voxel-level alpha = .001, uncorrected).

Relationship between anxiety scores and neural responses

An important goal of the present study was to understand the link between participants' anxiety scores and brain responses at cue and target phases. For the cue phase, we ran a voxel-wise across-subject robust regression analysis between differential threat vs. safe responses and participants' anxiety scores (separately for state and trait scores). Here, as in other analyses, we employed iterative reweighted least squares (the robustfit function from Matlab, Mathworks, Natick, MA, USA), given that standard Pearson correlation is very sensitive to even a few influential data points (Wilcox, 2005; see also Wager et al., 2005); results from robust regression are reported in terms of R^2. We restricted this analysis to regions that showed greater cue responses during the threat vs. safe condition because we were interested in how individual differences in anxiety influenced these responses.

For the target phase, we were interested in evaluating the link between individual differences in anxiety scores and *Monitoring* x *Interference* interaction-related responses. Accordingly, we ran a voxel-wise robust regression analysis involving each participant's interaction index *$(\text{incongruent} - \text{neutral})_{\text{THREAT}} - (\text{incongruent} - \text{neutral})_{\text{SAFE}}$] and anxiety scores. This analysis was restricted to brain regions that exhibited a main effect of *interference* (i.e., collapsed across safe and threat conditions; except the fusiform gyrus, which was targeted via the localizer-related analysis and the cerebellum, for which we did not have a clear hypothesis), so that we could assess the impact of individual differences in anxiety on these responses. Note that given that the main effect of interference is orthogonal to the interaction term, no circularity was incurred in the analysis (Kriegeskorte et al., 2009).

As before, the thresholds for voxelwise statistical tests was adjusted by Monte-Carlo simulations using the 3dClustSim program of the AFNI toolkit (cluster-level alpha = .05; cue-phase cluster extent: 3; target-phase cluster extent: 4; voxel-level alpha = .001, uncorrected).

Mediation analysis

To test the model displayed on Fig. 8, we performed mediation analysis (Baron and Kenny, 1986). The model formalizes the hypothesis that individual differences in state anxiety are linked to the level of threat-related response during the cue phase, thereby determining the extent of conflict-related responses during the subsequent target phase. A standard statistical approach was adopted, which involved evaluating the following components: (1) total effect *c* (initial variable → outcome, which can also be written in terms of the indirect effect *ab* plus the direct effect *c*′), (2) indirect path *a* (initial variable → intervening variable), (3) indirect path *b* (intervening variable → outcome after controlling for the initial variable), and (4) direct effect *c*′ (initial variable → outcome after controlling for the intervening

variable). The final mediation effect was tested by assessing the significance of the product of paths *a* and *b* (see Fig. 8) by using a bootstrapping procedure as implemented in the mediation toolbox by Tor Wager (http://wagerlab.colorado.edu/files/tools/mediation.html).

State anxiety scores across participants were employed as the initial variable in the mediation analysis. For the mediator variable, cue-related responses from the medial PFC and the right thalamus were employed (in separate analyses). Target responses in the left anterior insula comprised the outcome variable. Because we were interested in evaluating how threat-related processing during cue affected target-related responses, indices based on differential responses were employed (see Fig. 8). Specifically, differential responses between safe and threat were used during the cue phase and an interaction-type index was employed during the target phase. In particular, the interaction term measured how interference-related processing (incongruent vs. neutral) varied with threat of shock.

The mediation analysis was performed in terms of regions of interest (ROI). For the target phase, the left anterior insula ROI consisted of voxels that showed a significant linear association between state anxiety scores and changes in interference-related responses as a function of threat (i.e., an interaction). For the cue phase, we investigated two ROIs as potential mediators: medial PFC and right thalamus. Both ROIs comprised voxels that showed increased threat vs. safe responses and whose differential responses were linearly related with state anxiety scores. For each ROI, we averaged the regression coefficients of all the voxels to create a representative set of estimates (5-mm radius). A single medial PFC ROI was used given that voxels were situated very close to the midline and spanned both hemispheres (x = 1; y = 8; z = 32).

Because the ROIs chosen to test the mediation model were selected based on information related to state anxiety, one may question whether the procedure outlined above (see Fig. 8) is circular (Kriegeskorte et al., 2009). Note, however, that the estimation of the path coefficient *b* (relationship between mediation variable, M, and outcome variable, Y) is done by controlling for the effect of × (state anxiety). Nevertheless, we ran additional simulations to evaluate if any bias was incurred by the selection procedure. We simulated the selection procedure by generating 1,500 Gaussian-distributed random samples with mean and standard deviation based on actual medial PFC data. Importantly, the random samples were chosen so as to exhibit correlation values with state anxiety that were similar to that observed with actual data (actual data: $r = .40$; range of random samples: $r = .36$ to .44). Our simulation results revealed a false positive rate of only 1.1%, which demonstrates that our selection procedure does not inappropriately inflate Type I error rate.

Definition of regions of interest (ROIs) in visual cortex

ROIs in visual cortex, namely bilateral parahippocampal gyrus and left fusiform gyrus, were defined based on data from the localizer run. These ROIs were defined at the subject level via the contrast of word vs. scene blocks. Specifically, for the left fusiform gyrus, voxels were considered that exhibited stronger responses for word relative to scene blocks ($p < .005$, uncorrected); for the parahippocampal gyrus, the reverse contrast was employed. In both cases, a 5-mm radius sphere centered on the peak voxel was used. Mean coordinates for the ROIs were as follows: left fusiform gyrus: x = −42, y = −43, z = −14; left parahippocampal gyrus: x = −27, y = −45, z = −6; right parahippocampal gyrus: x = 26, y = −44, z = −7. We could not collect the localizer run data from two participants and we were not able to localize the left fusiform gyrus of one of the participants; thus, the corresponding analysis included data from 38 participants.

Connectivity analysis during cue phase

As discussed in the Introduction, the medial PFC is an important region during threat processing. To investigate how the medial PFC interacted with other brain regions during shock anticipation, we performed trial-by-trial functional connectivity analysis. We employed methods originally described by D'Esposito and colleagues (Rissman et al., 2004), which we have successfully employed in the past (Padmala and Pessoa, 2011). For each participant, we estimated the responses for each trial during the cue and target phases. Specifically, for each participant, a design matrix was set up such that each trial's cue and target phase were coded as separate events. To provide response estimates for the cue and target phases of each trial, a hemodynamic response was assumed (Cohen, 1997). Although in so doing we assumed that evoked responses were transient (which may not have been the optimal assumption for some brain regions during cue processing), overall, trial-based estimates provided good fits to the data (R^2 = .59, mean value across participants at the peak voxel in medial PFC). For an evaluation of this method in the context of functional connectivity analysis, see Zhou et al. (2009). Note that without assuming a fixed shape, the estimation of single-trial responses during relatively fast-paced event-related designs is poor, and possibly unfeasible.

Medial PFC ROIs were defined based on the contrast of threat vs. safe condition (ROIs on the left and right hemispheres were defined given that independent activation clusters were observed; left: x = −4; y = 5; z = 32; right: x = 11; y = 5; z = 38). A 5-mm radius sphere centered on the peak voxel of the contrast was used (see Table 2). Trial-based responses were averaged across all voxels within an ROI to create representative estimates. The linear relationship between trial-by-trial responses in the medial PFC ROIs (separately for right and left ROIs) and voxels within a restricted search space (defined via the contrast threat > safe during the cue phase; $p < .05$, cluster level) was evaluated with robust regression analysis. Regression coefficients were estimated for the threat and safe conditions, separately, and compared at the group level via a paired *t* test. As before, the threshold for voxelwise statistical tests was adjusted by Monte-Carlo simulations using the 3dClustSim program of the AFNI toolkit (cluster-level *p* value of .05; individual voxels: $p < .001$, uncorrected).

Concerning potential circularity in the connectivity analysis, note that both medial PFC and the restricted voxel search space were defined based on "average" threat vs. safe responses (as assessed via a paired *t* test), whereas the functional connectivity analysis involved trial-by-trial analysis. For each condition, trial-by-trial fluctuations are independent from mean-level responses, thus avoiding circularity in the procedure.

Results

Skin Conductance Responses

Skin conductance responses revealed that responses were greater during trials involving shock monitoring relative to safe ones [mean (STD) in log-transformed units: .019 (.019) during threat and .003 (.009) during safe]. Indeed, a paired *t* test revealed a significant difference (t_{37} = 4.53, $p < .001$), indicating that the shock manipulation was successful.

Behavioral results

Reaction time data (Fig. 2A) were evaluated according to a 2 *Monitoring* (safe, threat) x 3 *Congruency* (neutral, congruent, incongruent) repeated–measures ANOVA. The main effect of *Anticipation* was not significant ($F_{1, 40}$ = .14, p = .7130), whereas a significant main effect of *Congruency* was detected ($F_{2, 80}$ = 42.42, $p < .0001$). As expected, mean RT was longest on incongruent trials (744 ms), shortest on congruent trials (690 ms), and

intermediate on neutral trials (696 ms). Notably, a statistically significant *Monitoring* x *Congruency* interaction was obtained ($F_{2, 80} = 5.02$, $p = .0089$).

To further investigate the data, we conducted an additional 2 × 2 ANOVA. As in the neuroimaging data below, we focused on incongruent-trial effects because they inform about interference processing. We included congruent trials in the design because, without them, interference is substantially reduced (Lowe and Mitterer, 1982; Besner et al., 1997). But the interpretation of congruent trials is less straightforward, as they may also engender increased competition relative to neutral trials, in the sense that two sources of information need to be dealt with (although both lead to the correct response). For a more extended discussion of this issue, please refer to Posner and DiGirolamo (1998) and Milham et al. (2002).

The *Monitoring* (safe, threat) x *Interference* (neutral, incongruent) ANOVA did not reveal a main effect of *Monitoring* ($F_{1, 40} = .04$, $p = .8409$), but a significant main effect of *Interference* ($F_{1, 40} = 42.91$, $p < .0001$) and interaction ($F_{1, 40} = 6.57$, $p = .0142$) were obtained. Specifically, interference was observed both during the safe (incongruent – neutral RT: mean: 35 ms, STD: 54.57; $t_{40} = 4.15$, $p = .0002$) and threat (incongruent – neutral RT: mean: 60 ms, STD: 56.92; $t_{40} = 6.74$, $p < .0001$) conditions, but was larger in the latter, indicating that participants found incongruent trials more challenging when a shock was anticipated during the delay period.

Next, we examined the relationship between individual anxiety levels and interaction scores (i.e., how interference changed as a function of individual differences). Robust regression analysis showed a significant positive linear relationship between the two ($R^2 = .17$, $p = .0333$), indicating that the interference difference ($[\text{incongruent} - \text{neutral}]_{\text{THREAT}} - [\text{incongruent} - \text{neutral}]_{\text{SAFE}}$) increased with state anxiety (Fig. 2B). This relationship was not observed with trait anxiety ($R^2 = .04$, $p = .3804$).

It is valuable to consider if the 2 *Monitoring* x 2 *Interference* interaction and the positive linear relationship with state anxiety were driven by the neutral condition. To do so, RTs on safe and threat trials were contrasted separately for the neutral and incongruent conditions, and revealed only modest *t* values (neutral trials: $t_{40} = 1.76$, $p = .0858$; incongruent trials: $t_{40} = 1.62$, $p = .1138$). Notably, however, robust regression analyses revealed a significant positive linear relationship of differential scores (threat – safe) with state anxiety during the incongruent condition ($R^2 = .18$, $p = .0086$), but not during the neutral condition ($R^2 = .02$, $p = .4201$). Therefore, whereas neutral trials contributed to the 2 × 2 interaction, importantly, the relationship with state anxiety was only robustly driven by threat.

Similar analyses were performed for error rate data. A 2 *Monitoring* (safe, threat) x 3 *Congruency* (neutral, congruent, incongruent) repeated-measures ANOVA revealed that the main effect of *Monitoring* was not significant ($F_{1, 40} = .11$, $p = .7390$), whereas a main effect of congruency was observed ($F_{2, 80} = 35.41$, $p < .0001$). Errors were most frequent during incongruent trials (10.08 %), least frequent during congruent trials (4.09 %), and intermediate during neutral trials (5.21 %). Notably, a statistically significant *Monitoring* x *Congruency* interaction was obtained ($F_{2, 80} = 5.78$, $p = .0045$). As in the RT data, a subsequent 2 *Monitoring* (safe, threat) x *Interference* (neutral, incongruent) repeated-measures ANOVA revealed both a significant interaction ($F_{1, 40} = 11.68$, $p = .0015$) and main effect of *Interference* ($F_{1, 40} = 35.03$, $p < .0001$), but no main effect of *Monitoring* ($F_{1, 40} = .12$, $p = .7297$). Again, the amount of interference (incongruent – neutral) increased during the threat (6.64 %) relative to the safe (3.10 %) condition. Finally, a regression analysis did not reveal evidence for an association between state or trait anxiety and interaction scores based on error rates.

Functional MRI results

Target phase—An important goal of this study was to investigate how interference-related processing is influenced by the threat of shock. Given our behavioral analysis, initially we ran a 2 *Monitoring* (safe, threat) × 2 *Interference* (neutral, incongruent) voxelwise repeated-measures ANOVA, which revealed a significant main effect of *Interference* (incongruent > neutral) in several fronto-parietal regions, including medial prefrontal cortex, bilateral anterior insula, and bilateral intraparietal sulcus (Fig. 3A; Table. 1). Significant main effects of *Monitoring* or *Monitoring* x *Interference* interactions were not detected.

Although this lack of an interaction result was surprising, we reasoned that it was not detected possibly due to the influence of anxiety levels. In other words, the effect of threat on interference processing depended itself on individual differences in state anxiety – thus, anxiety potentially "masked" the interaction. For instance, an *Monitoring* x *Interference* interaction would be evident for high- but not for low-anxious individuals. This relationship could be formally tested by dichotomizing participants into low- and high-anxious groups and testing for a three-way interaction. In the presence of continuous data, dichotomization is a poor choice, however, and analyses that retain the continuous nature of the variable in question (i.e., state and trait anxiety scores) are preferable. Given these considerations, it is conceivable that regions with responses sensitive to state/trait anxiety would not reveal robust cognitive-emotional interactions (i.e., a two-way interaction) unless individual differences were explicitly incorporated. To probe this question, we followed the same strategy as in the behavioral data (see Fig. 2B). Initially, interaction-type scores were determined: $[(\text{incongruent} - \text{neutral})_{\text{THREAT}} - (\text{incongruent} - \text{neutral})_{\text{SAFE}}]$. Robust regression was then employed to assess the linear relationship between interaction scores and state anxiety, which revealed a positive link in the left anterior insula ($R^2 = .18$; Fig. 3B). Follow-up analyses revealed that this relationship was driven by the threat condition. Specifically, a statistically significant linear relationship was observed between $(\text{incongruent} - \text{neutral})_{\text{THREAT}}$ and state anxiety ($R^2 = .24$), but not between $(\text{incongruent} - \text{neutral})_{\text{SAFE}}$ and state anxiety ($R^2 < .01$). These analyses indicate that individual differences in state anxiety are specifically related to how interference resolution is affected by the preceding anticipation of shock.

Cue phase—Next, we probed responses evoked during the cue phase by comparing threat and safe conditions. Note that because the cue was always followed by the delay period, no attempt was made to separate cue responses from those related to the delay period (see Methods). Indeed, although we refer to the responses estimated with respect to cue onset as "cue related", they likely combined these components. However, as desired, the estimation of "cue" responses was independent of the target phase (for further discussion, see Padmala and Pessoa, 2011).

Stronger responses to threat were observed across fronto-parietal cortex, including bilateral inferior parietal gyrus, medial PFC, bilateral anterior insula, and right thalamus (Fig. 4A; Table 2). Given the suggested role of the BNST in "extended fear" (Davis et al., 2010), it is noteworthy that a site consistent with the right BNST abutting the caudate exhibited greater responses to threat vs. safe (threat > safe; Fig. 7). At an exploratory threshold of .001 (uncorrected), we observed similar responses in the left BNST/caudate.

Extensive activation was also observed in the reverse direction, namely safe greater than threat, and appeared to overlap with the pattern associated with the task-negative ("resting-state") network (Fox et al., 2005; Fig. 5). In our task, responses in the amygdala were of particular interest given the role of this structure in threat processing. Unexpectedly, during the cue phase, we observed greater responses to the safe relative to the threat condition (Fig.

6). Note, however, that habituation does not explain this result because cue-related responses during the threat condition did not differ significantly between the first and second halves of the experiment (left amygdala: $t_{40} = -1.49$, $p = .1441$; right amygdala: $t_{40} = -1.34$, $p = .1878$). Furthermore, responses in the amygdala during actual shock trials exhibited a fairly canonical shape (Fig. 6B), indicating that signal quality in this region was adequate.

Were cue-related responses associated with state anxiety? To probe this question, voxels exhibiting greater activation during threat relative to safe were interrogated. Robust regression analysis identified negative relationships between differential cue-related responses and state anxiety in the medial PFC ($R^2 = .16$) and right thalamus ($R^2 = .38$) (Fig. 4B and 4C). For the medial PFC, the relationship was detected during the threat condition when probed by itself ($R^2 = .08$) but not during the safe condition when probed by itself ($R^2 < .01$). Likewise, for the right thalamus, the relationship was detected reliably during the threat condition ($R^2 = .13$), but not during the safe condition ($R^2 < .01$). These results show that state anxiety levels had a specific effect on cue processing when it signaled threat.

Mediation

Given that a link between state anxiety scores and interaction-type responses (i.e., *Monitoring* x *Interference*) was observed in the left anterior insula during the target phase, we investigated the role of cue-related activation sites as potential mediators of the relationship (Fig 8). To do so, we focused on the medial PFC and the right thalamus, as differential responses in these areas were correlated with state anxiety scores. A mediation analysis revealed that the relationship between participants' state anxiety levels and left anterior insula responses during the target phase was partially mediated by cue responses in medial PFC, but not the right thalamus (Table 3). In other words, the direct effect between state anxiety scores and left anterior insula interaction scores was significantly reduced once the contribution of the medial PFC was taken into account – a relationship that was evaluated by assessing the product of path weights *a* and b ($ab = .14$, $t_{40} = 1.38$, $p = .028$).

Visual responses during the target phase in category-responsive regions

We investigated category-related responses in inferior temporal cortex, including those in the left fusiform gyrus, which responds more strongly to word stimuli, and in the parahippocampal gyrus, bilaterally, which responds more strongly to scene stimuli. Target-related responses were investigated in ROIs defined based on localizer runs according to a 2 *Monitoring* (safe, threat) × 2 *Interference* (neutral, incongruent) repeated-measures ANOVA. In the left fusiform gyrus, a significant main effect of *Interference* was observed ($F_{1,37} = 25.70$, $p < .001$); the main effect of *Monitoring* ($F_{1,37} < .01$, $p = .949$) and the *Monitoring* x *Interference* interaction ($F_{1,37} = .91$, $p = .345$) were not detected. As done previously, we probed whether interaction-type scores [$(\text{incongruent} - \text{neutral})_{\text{THREAT}} - (\text{incongruent} - \text{neutral})_{\text{SAFE}}$] were linearly related to state anxiety. Robust regression revealed a positive link in the left fusiform gyrus ($R^2 = .12$, $p = .032$). Follow-up analyses revealed that this relationship was driven by the threat condition. Specifically, a significant linear relationship was observed between $(\text{incongruent} - \text{neutral})_{\text{THREAT}}$ and state anxiety ($R^2 = .17$, $p = .010$), but not between $(\text{incongruent} - \text{neutral})_{\text{SAFE}}$ and state anxiety ($R^2 = .01$, $p = .207$). In the Discussion, we suggest that a possible interpretation of these results is in terms of how distractor (i.e., word) processing is affected by threat, task condition, and state anxiety. Significant effects were not detected in the parahippocampal gyri (all $Fs_{1,37} < 2.26$, all $ps > .141$).

Functional connectivity during cue phase

As discussed in the Introduction, the medial PFC is an important region during threat processing. To investigate how the medial PFC interacted with other brain regions during

shock anticipation, we performed trial-by-trial functional connectivity analysis. Accordingly, we estimated single-trial, cue-related responses separately during the safe and threat conditions and evaluated the linear association between the medial PFC and other regions (specifically, voxels exhibiting stronger responses to threat vs. safe). Across subjects, the strength of the relationship between the left medial PFC and the right thalamus (x=8, y=−13, z=2; Fig. 9A and 9B) increased during threat relative to safe; the strength also increased between the right medial PFC and the left anterior insula (x=−28, y=20, z=−4; Fig. 9A and 9C).

Discussion

In the present study, we investigated how threat affected subsequent response-conflict processing. Behaviorally, a threat monitoring by response conflict interaction was observed in that interference (incongruent vs. neutral RT) was increased following threat monitoring. These interaction effects were positively related to state anxiety scores across individuals – the higher the state anxiety, the larger the interference during the threat condition. The neuroimaging findings also revealed effects of threat during both the cue and target phases that were modulated by individual differences in state anxiety. Furthermore, the influence of state anxiety on the extent of interaction effects during the target phase was partially mediated via responses in the medial PFC during the cue phase. In the following, we discuss our findings at greater length.

Behaviorally, monitoring for a mild shock increased the amount of subsequent response interference, consistent with findings that emotion interferes with cognitive performance, especially when the task is more effortful – as when conflict needs to be resolved during incongruent trials. The pattern of behavioral results is also consistent with the idea that threat processing consumes processing resources required for executive control, much like other more phasic emotional manipulations (Pessoa, 2009); but see Hu et al., (2011). Notably, RT interaction effects were positively associated with state anxiety. Thus, participants with higher state anxiety levels showed greater interference during threat (relative to safe). The effect of individual differences in anxiety on cognitive performance has been extensively documented in non-emotional tasks (Eysenck and Calvo, 1992; Eysenck et al., 2007; Bishop, 2009). Effects in tasks involving emotional stimuli have also been reported, such as the emotional Stroop task in which high-anxious participants showed slower responses to stimuli containing threat relative to neutral words (Williams et al., 1996; Koven et al., 2003).

Brain responses were first investigated at the target phase. Stronger responses to incongruent vs. neutral trials were observed in multiple fronto-parietal sites, including medial PFC, middle frontal gyrus, and anterior insula. No threat by conflict interactions were detected. However, given the behavioral results, we were particularly interested in examining how interaction scores [$(\text{incongruent} - \text{neutral})_{\text{THREAT}} - (\text{incongruent} - \text{neutral})_{\text{SAFE}}$] were linked to state anxiety. Our analysis revealed a positive relationship between the two in the left anterior insula – indicating that the influence of threat on interference-related responses was greater for subjects with higher state anxiety. The confluence of effects of cognitive task condition, threat processing, and state anxiety in the anterior insula is particularly noteworthy given the importance of this region in both emotion and cognition. Whereas the importance of the anterior insula for affective processing is well established (Mesulam, 2000), this region appears to be a core region of the executive control system, too (Dosenbach et al., 2006; Van Snellenberg and Wager, 2009). In two other regions widely reported to be involved in cognitive control, namely medial PFC and lateral PFC, we observed a significant main effect of interference (incongruent vs. neutral), but did not observe a significant threat monitoring by response interference interaction, or a relationship

between interaction scores and individual differences in state anxiety. The negative findings concerning the medial PFC were surprising given that this region is engaged during response interference (Botvinick et al., 2001) – indeed, we had anticipated an interaction in this region as described in the Introduction.

As in the case of the left anterior insula, during the target phase, state anxiety scores also showed a positive linear relationship with interaction scores in the left fusiform gyrus (defined via a separate localizer). Given the role of the left fusiform gyrus in word processing (Polk and Farah, 2002; McCandliss et al., 2003), the contrast of incongruent vs. neutral stimuli may be seen as providing an index of word processing in this region, as only the former condition involved a word. It is thus conceivable that the pattern of results observed reflected a modulation of state anxiety on the extent of distractor-related (i.e., word-related) processing during the threat condition.

During the cue phase, stronger responses to threat relative to safe were observed in medial PFC, bilateral anterior insula, and right thalamus, among other regions. As previously noted, because the cue was always followed by the delay period, no attempt was made to separate the two – although we refer to the responses estimated with respect to cue onset as “cue related”, they likely combined these components to some extent. Several studies have implicated these regions during the anticipation of aversive events (Chua et al., 1999; Ploghaus et al., 1999; Simmons et al., 2006). In particular, the medial PFC and thalamus are involved in the regulation of anxiety-related behaviors in non-human primates (Kalin et al., 2005). Human neuroimaging studies have described the engagement of the medial PFC (Banks et al., 2007; for review Ochsner and Gross, 2005) and thalamus (Herwig et al., 2007; Goldin et al., 2008) in emotion regulation, too. In the present study, during the cue phase, we observed a negative linear relationship between state anxiety scores and differential responses (threat vs. safe) in both medial PFC and right thalamus. Given the role of the medial PFC and thalamus (Kalin et al., 2005; Herwig et al., 2007; Goldin et al., 2008) in emotion regulation, it is conceivable that the negative relationship reflected the relatively poorer ability of high-anxious individuals to regulate affective responses during shock anticipation. It is noteworthy that the negative relationship was present in the threat condition but not in the safe condition (when the conditions were probed individually), suggesting that the pattern was specific to threat.

As described above, state anxiety was positively related to the increase in target-phase interference-related responses in the left anterior insula during the threat condition. As threat and safe trials were identical except for the cue stimulus, we performed a path analysis to test for potential mediators during the cue phase (Fig. 8). This analysis revealed a partial mediation via the medial PFC. Participants with higher state anxiety showed decreased differential cue-related responses in medial PFC (path a), consistent with the idea that more anxious individuals had difficulty in engaging the medial PFC during the threat condition. At the same time, smaller threat-related responses in the medial PFC during the cue phase were observed in conjunction with increased interference-related responses in the left anterior insula during the target phase (path b), consistent with the idea that the poor engagement of the medial PFC during threat impaired cognitive control during response conflict in the left anterior insula.

As described previously, during cue processing, several regions were engaged more strongly during threat relative to safe. Because several of these regions have been implicated in threat or aversive-stimulus anticipation in the past (Kalin et al., 2005; Chandrasekhar et al., 2008; Mobbs et al., 2010), we reasoned that they might work as a network of regions during these conditions. To evaluate this possibility, we performed a functional connectivity analysis and used the medial PFC as a “seed” region (separately for the left and right hemispheres). Trial-

by-trial responses in the left medial PFC were more strongly correlated with those in the right thalamus during threat vs. safe. Likewise, trial-by-trial responses in the right medial PFC were more strongly correlated with those in the left anterior insula during threat vs. safe. These findings reveal that during threat monitoring, not only are regions such as medial PFC, anterior insula, and thalamus more strongly engaged, but their responses are more strongly coupled (i.e., responses are more similar), consistent with the notion that they function as a network.

Whereas the contrast direction “threat > safe” revealed activation in a discrete set of regions, the reverse contrast direction “safe > threat” was associated with widespread brain responses. Interestingly, the pattern of activation overlapped considerably with the task-negative network, namely, those regions that robustly exhibit decreased activation during effortful task execution (relative to rest). It thus appears that the threat cue robustly engaged brain regions that are part of the task-negative network (i.e., it appeared to “deactivate” these regions). Related findings were reported by Simpson et al. (2001), who found decreased responses in ventral regions of medial PFC when participants were anticipating a shock.

Finally, given the important role played by the amygdala in fear and threat processing, we were interested in how it responded during the cue phase. Surprisingly, relative to safe, the amygdala appeared to be deactivated during threat, a pattern that is unlike the one commonly observed to CS+ (vs. CS−) stimuli in aversive conditioning studies (Büchel et al., 1998; LaBar et al., 1998; Lim et al., 2009); note, however, that SCRs were greater to threat vs. safe. Whereas the reasons for the difference are unclear, we offer the following speculative account. Responses in the amygdala may be more closely tied to phasic cue stimuli. In the present study, the geometric-shaped cues signaled a variable-length delay period during which a shock could be administered at any time. Although our delays were relatively short in duration (1.75–5.75 s), they comprised a period of shock anticipation that may have triggered neuronal mechanisms that are distinct from those typically associated with aversive conditioning studies. Indeed, our paradigm may have been closer to those labeled anxiety (as opposed to fear) by Davis, Grillon, and colleagues – situations involving more temporally extended and less predictable threats. This possibility prompted us to investigate basal forebrain sites consistent with the bed nucleus of the stria terminalis, a structure that has been implicated in such anxiety-related mechanisms (Davis et al., 2010). In a region consistent with the BNST/caudate, stronger responses were observed during threat relative to safe. In the present context, it is noteworthy that Somerville and colleagues (2010) also did not detect amygdala responses during threat monitoring that occurred over a more temporally extended period.

In conclusion, our study revealed threat monitoring by response conflict interactions both at the behavioral and neural levels. Behaviorally, threat increased response interference. In the brain, a parallel pattern was observed, but was moderated by state anxiety – only high-anxious individuals exhibited increased interference-related responses during threat. Notably, this relationship was observed in the anterior insula, a structure that may be particularly important for the interaction between emotion and cognition.

References

Anticevic A, Repovs G, Barch DM. Resisting emotional interference: Brain regions facilitating working memory performance during negative distraction. Cognitive, Affective, & Behavioral Neuroscience. 2010; 10:159–173.

Bach DR, Flandin G, Friston KJ, Dolan RJ. Time-series analysis for rapid event-related skin conductance responses. Journal of Neuroscience Methods. 2009; 184:224–234. [PubMed: 19686778]

Banks SJ, Eddy KT, Angstadt M, Nathan PJ, Phan KL. Amygdala–frontal connectivity during emotion regulation. Social Cognitive and Affective Neuroscience. 2007; 2:303–312. [PubMed: 18985136]

Baron RM, Kenny DA. The moderator–mediator variable distinction in social psychological research: Conceptual, strategic, and statistical considerations. Journal of personality and social psychology. 1986; 51:1173–1182. [PubMed: 3806354]

Besner D, Stolz JA, Boutilier C. The stroop effect and the myth of automaticity. Psychon Bull Rev. 1997; 4:221–225. [PubMed: 21331828]

Bishop SJ. Trait anxiety and impoverished prefrontal control of attention. Nat Neurosci. 2009; 12:92–98. [PubMed: 19079249]

Blair KS, Smith BW, Mitchell DGV, Morton J, Vythilingam M, Pessoa L, Fridberg D, Zametkin A, Nelson EE, Drevets WC. Modulation of emotion by cognition and cognition by emotion. NeuroImage. 2007; 35:430–440. [PubMed: 17239620]

Botvinick MM, Braver TS, Barch DM, Carter CS, Cohen JD. Conflict monitoring and cognitive control. Psychological Review. 2001; 108:624–652. [PubMed: 11488380]

Brown JW, Braver TS. Learned predictions of error likelihood in the anterior cingulate cortex. Science. 2005; 307:1118–1121. [PubMed: 15718473]

Büchel C, Morris J, Dolan RJ, Friston KJ. Brain systems mediating aversive conditioning: an event-related fMRI study. Neuron. 1998; 20:947–957. [PubMed: 9620699]

Chandrasekhar PVS, Capra CM, Moore S, Noussair C, Berns GS. Neurobiological regret and rejoice functions for aversive outcomes. NeuroImage. 2008; 39:1472–1484. [PubMed: 18042401]

Chua P, Krams M, Toni I, Passingham R, Dolan R. A functional anatomy of anticipatory anxiety. NeuroImage. 1999; 9:563–571. [PubMed: 10334900]

Cohen MS. Parametric Analysis of fMRI Data Using Linear Systems Methods. NeuroImage. 1997; 6:93–103. [PubMed: 9299383]

Cox RW. AFNI: software for analysis and visualization of functional magnetic resonance neuroimages. Computers and Biomedical Research. 1996; 29:162–173. [PubMed: 8812068]

Cox RW, Jesmanowicz A. Real-time 3D image registration for functional MRI. Magnetic resonance in medicine. 1999; 42:1014–1018. [PubMed: 10571921]

Craig AD. How do you feel? Interoception: the sense of the physiological condition of the body. Nat Rev Neurosci. 2002; 3:655–666. [PubMed: 12154366]

Craig AD. How do you feel--now? The anterior insula and human awareness. Nat Rev Neurosci. 2009; 10:59–70. [PubMed: 19096369]

Davis M, Walker DL, Miles L, Grillon C. Phasic vs sustained fear in rats and humans: role of the extended amygdala in fear vs anxiety. Neuropsychopharmacology. 2010; 35:105–135. [PubMed: 19693004]

Dolcos F, McCarthy G. Brain systems mediating cognitive interference by emotional distraction. J Neurosci. 2006; 26:2072–2079. [PubMed: 16481440]

Dosenbach NU, Visscher KM, Palmer ED, Miezin FM, Wenger KK, Kang HC, Burgund ED, Grimes AL, Schlaggar BL, Petersen SE. A core system for the implementation of task sets. Neuron. 2006; 50:799–812. [PubMed: 16731517]

Epstein R, Harris A, Stanley D, Kanwisher N. The Parahippocampal Place Area:: Recognition, Navigation, or Encoding? Neuron. 1999; 23:115–125. [PubMed: 10402198]

Eysenck MW, Calvo MG. Anxiety and performance: The processing efficiency theory. Cognition and Emotion. 1992; 6:409–434.

Eysenck MW, Derakshan N, Santos R, Calvo MG. Anxiety and cognitive performance: Attentional control theory. Emotion. 2007; 7:336–353. [PubMed: 17516812]

Fox MD, Snyder AZ, Vincent JL, Corbetta M, Van Essen DC, Raichle ME. The human brain is intrinsically organized into dynamic, anticorrelated functional networks. Proceedings of the National Academy of Sciences of the United States of America. 2005; 102:9673–9678. [PubMed: 15976020]

Goldin PR, McRae K, Ramel W, Gross JJ. The neural bases of emotion regulation: Reappraisal and suppression of negative emotion. Biological Psychiatry. 2008; 63:577–586. [PubMed: 17888411]

Hart SJ, Green SR, Casp M, Belger A. Emotional priming effects during Stroop task performance. NeuroImage. 2010; 49:2662–2670. [PubMed: 19883772]

Herwig U, Baumgartner T, Kaffenberger T, Brühl A, Kottlow M, Schreiter-Gasser U, Abler B, Jäncke L, Rufer M. Modulation of anticipatory emotion and perception processing by cognitive control. NeuroImage. 2007; 37:652–662. [PubMed: 17588776]

Hu K, Bauer A, Padmala S, Pessoa L. Threat of bodily harm has opposing effects on cognition. Emotion. 2011 (in press).

Kalin NH, Shelton SE, Fox AS, Oakes TR, Davidson RJ. Brain regions associated with the expression and contextual regulation of anxiety in primates. Biological Psychiatry. 2005; 58:796–804. [PubMed: 16043132]

Kanske P, Kotz SA. Emotion Speeds up Conflict Resolution: A New Role for the Ventral Anterior Cingulate Cortex? Cerebral Cortex. 2010; 21:911–919. [PubMed: 20732901]

Koven NS, Heller W, Banich MT, Miller GA. Relationships of distinct affective dimensions to performance on an emotional Stroop task. Cognitive Therapy and Research. 2003; 27:671–680.

Kriegeskorte N, Simmons WK, Bellgowan PSF, Baker CI. Circular analysis in systems neuroscience: the dangers of double dipping. Nature Neuroscience. 2009; 12:535–540.

LaBar KS, Gatenby JC, Gore JC, LeDoux JE, Phelps EA. Human amygdala activation during conditioned fear acquisition and extinction: a mixed-trial fMRI study. Neuron. 1998; 20:937–945. [PubMed: 9620698]

Lim SL, Padmala S, Pessoa L. Segregating the significant from the mundane on a moment-to-moment basis via direct and indirect amygdala contributions. Proceedings of the National Academy of Sciences. 2009; 106:16841–16846.

Loftus GR, Masson ME. Using confidence intervals in within-subject designs. Psychonomic Bulletin & Review. 1994; 1:476–490.

Lowe DG, Mitterer JO. Selective and divided Attention in a Stroop task. Can J Psychol. 1982; 36:684–700. [PubMed: 7159848]

McCandliss BD, Cohen L, Dehaene S. The visual word form area: expertise for reading in the fusiform gyrus. Trends in Cognitive Sciences. 2003; 7:293–299. [PubMed: 12860187]

Mesulam, MM. Principles of behavioral and cognitive neurology. Oxford University Press; USA: 2000.

Milham MP, Erickson KI, Banich MT, Kramer AF, Webb A, Wszalek T, Cohen NJ. Attentional Control in the Aging Brain: Insights from an fMRI Study of the Stroop Task. Brain Cogn. 2002; 49:277–296. [PubMed: 12139955]

Mobbs D, Yu R, Rowe JB, Eich H, FeldmanHall O, Dalgleish T. Neural activity associated with monitoring the oscillating threat value of a tarantula. Proceedings of the National Academy of Sciences. 2010; 107:20582–20586.

Ochsner K, Gross J. The cognitive control of emotion. Trends in Cognitive Sciences. 2005; 9:242–249. [PubMed: 15866151]

Ollinger JM, Shulman GL, Corbetta M. Separating processes within a trial in event-related functional MRI. Neuroimage. 2001; 13:210–217. [PubMed: 11133323]

Padmala S, Pessoa L. Reward reduces conflict by enhancing attentional control and biasing visual cortical processing. Journal of Cognitive Neuroscience. 2011 (in press).

Pessoa L. How do emotion and motivation direct executive control? Trends in Cognitive Sciences. 2009; 13:160–166. [PubMed: 19285913]

Pessoa L, Padmala S, Kenzer A, Bauer A. Interactions between cognition and emotion during response inhibition. Emotion. 2011 (in press).

Ploghaus A, Tracey I, Gati JS, Clare S, Menon RS, Matthews PM, Rawlins JNP. Dissociating pain from its anticipation in the human brain. Science. 1999; 284:1979–1981. [PubMed: 10373114]

Polk TA, Farah MJ. Functional MRI evidence for an abstract, not perceptual, word-form area. Journal of Experimental Psychology: General. 2002; 131:65. [PubMed: 11900104]

Posner, MI.; DiGirolamo, GJ. Executive attention: Conflict, target detection, and cognitive control. In: Parasuraman, R., editor. The attentive brain. Cambridge, MA: MIT Press; 1998.

Prokasy, WF.; Raskin, DC. Electrodermal activity in psychological research. New York: Academic Press; 1974.

Rissman J, Gazzaley A, D'Esposito M. Measuring functional connectivity during distinct stages of a cognitive task. NeuroImage. 2004; 23:752–763. [PubMed: 15488425]

Ruge H, Goschke T, Braver TS. Separating event-related BOLD components within trials: The partial-trial design revisited. NeuroImage. 2009; 47:501–513. [PubMed: 19422920]

Simmons A, Strigo I, Matthews SC, Paulus MP, Stein MB. Anticipation of aversive visual stimuli is associated with increased insula activation in anxiety-prone subjects. Biological Psychiatry. 2006; 60:402–409. [PubMed: 16919527]

Simpson JR Jr, Drevets WC, Snyder AZ, Gusnard DA, Raichle ME. Emotion-induced changes in human medial prefrontal cortex: II. During anticipatory anxiety. Proc Natl Acad Sci U S A. 2001; 98:688–693. [PubMed: 11209066]

Somerville LH, Whalen PJ, Kelley WM. Human bed nucleus of the stria terminalis indexes hypervigilant threat monitoring. Biological Psychiatry. 2010; 68:416–424. [PubMed: 20497902]

Spielberger CD. State Trait Anxiety Inventory. 1970

Talairach, J.; Tournoux, P. Co-planar stereotaxis atlas of the human brain. New York: Thieme Medical; 1988.

Van Snellenberg, JX.; Wager, TD. Luria's legacy in the 21st century. 2009. Cognitive and motivational functions of the human prefrontal cortex; p. 30-61.

Wager TD, Keller MC, Lacey SC, Jonides J. Increased sensitivity in neuroimaging analyses using robust regression. NeuroImage. 2005; 26:99–113. [PubMed: 15862210]

Weissman DH, Gopalakrishnan A, Hazlett C, Woldorff M. Dorsal anterior cingulate cortex resolves conflict from distracting stimuli by boosting attention toward relevant events. Cerebral Cortex. 2005; 15:229–237. [PubMed: 15238434]

Wilcox, RR. Introduction to robust estimation and hypothesis testing. Academic Press; 2005.

Williams JMG, Mathews A, MacLeod C. The emotional Stroop task and psychopathology. Psychological Bulletin. 1996; 120:3–24. [PubMed: 8711015]

Zhou D, Thompson WK, Siegle G. MATLAB toolbox for functional connectivity. NeuroImage. 2009; 47:1590–1607. [PubMed: 19520177]

Highlights

- We investigated how shock monitoring affects subsequent conflict processing
- Interactions between shock monitoring and conflict processing were observed at both behavioral and neural levels
- Anticipating shock increased response conflict behaviorally, an effect that was influenced by individual differences in state anxiety
- Shock anticipation engaged the medial PFC, thalamus, anterior insula, and the bed nucleus of the stria terminalis
- An interaction between cognitive task condition, shock monitoring, and state anxiety was observed in the anterior insula

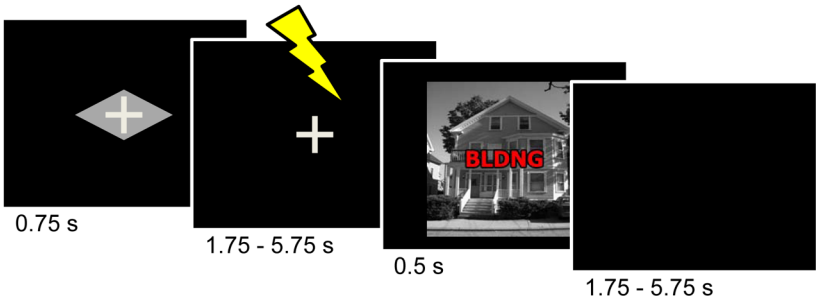

Figure 1.

Task design. Subjects performed a response-conflict task under two contexts, safe and threat. During the threat condition (shown here), a cue stimulus (diamond) signaled that a mild electric shock could occur during the delay period following cue offset and prior to the target display. Participants were instructed about the meaning of the cue stimuli prior to task execution. During the target phase, participants were asked to indicate whether the picture contained a house or a building, while ignoring the superimposed word. During the safe condition (not shown), the trial structure was identical, except for the shape of the cue stimulus (rectangle) and the fact that shocks were never administered.

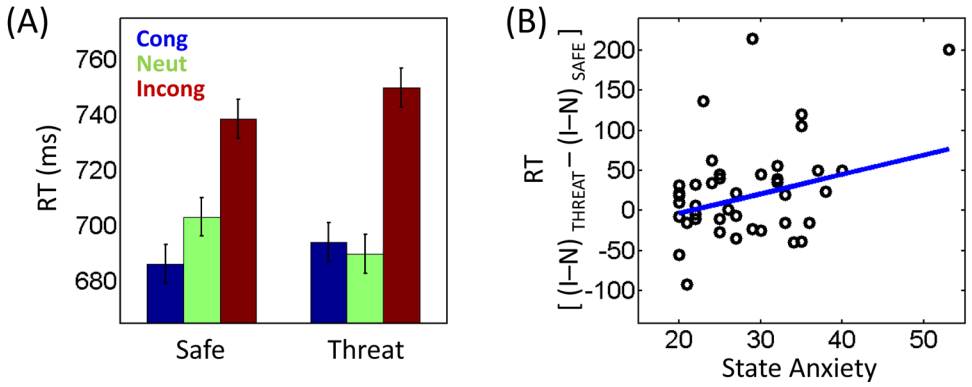

Figure 2.

Behavioral results. (A) Participants exhibited slower responses during incongruent trials. Importantly, the amount of interference (incongruent vs. neutral) was greater when the target display was preceded by a threat relative to safe cue. Cong, congruent trials; Neut, neutral trials; Incong, incongruent trials. (B) Across participants, interaction-type scores were linearly related to state anxiety levels. The blue line indicates the robust linear regression fit. I, incongruent trials; N, neutral trials. Error bars in panel A denote the standard within-subject error term (Loftus and Masson, 1994).

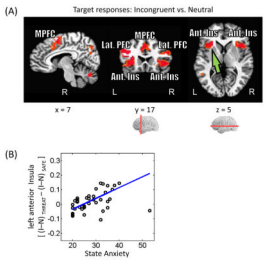

Figure 3.

Target-related responses. (A) Voxels that showed stronger responses during incongruent than neutral trials (displayed at $p < 0.05$, cluster-level corrected). MPFC, medial prefrontal cortex; Lat. PFC, lateral prefrontal cortex; Ant. Ins, anterior insula. (B) Across participants, interaction-type scores in the left anterior insula (see green arrow in panel A) were positively related to state anxiety levels. The blue line indicates the robust linear regression fit. I, incongruent trials; N, neutral trials.

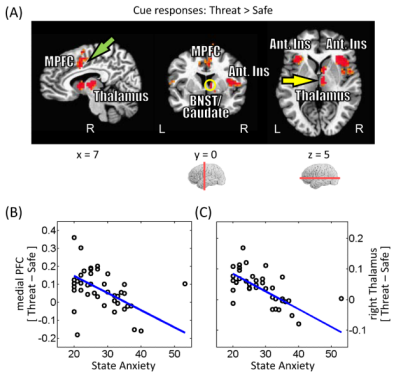

Figure 4.

Cue-related responses. (A) Voxels that showed stronger responses during threat than safe trials (displayed at $p < 0.05$, cluster-level corrected). MPFC, medial prefrontal cortex; BNST, bed nucleus of the stria terminalus (yellow circle); Ant. Ins, anterior insula. (B) Across participants, differential responses in the medial prefrontal cortex (see green arrow in panel A) were inversely related to state anxiety levels. The blue line indicates the robust linear regression fit. (C) As in (B) for the right thalamus (see yellow arrow in panel A).

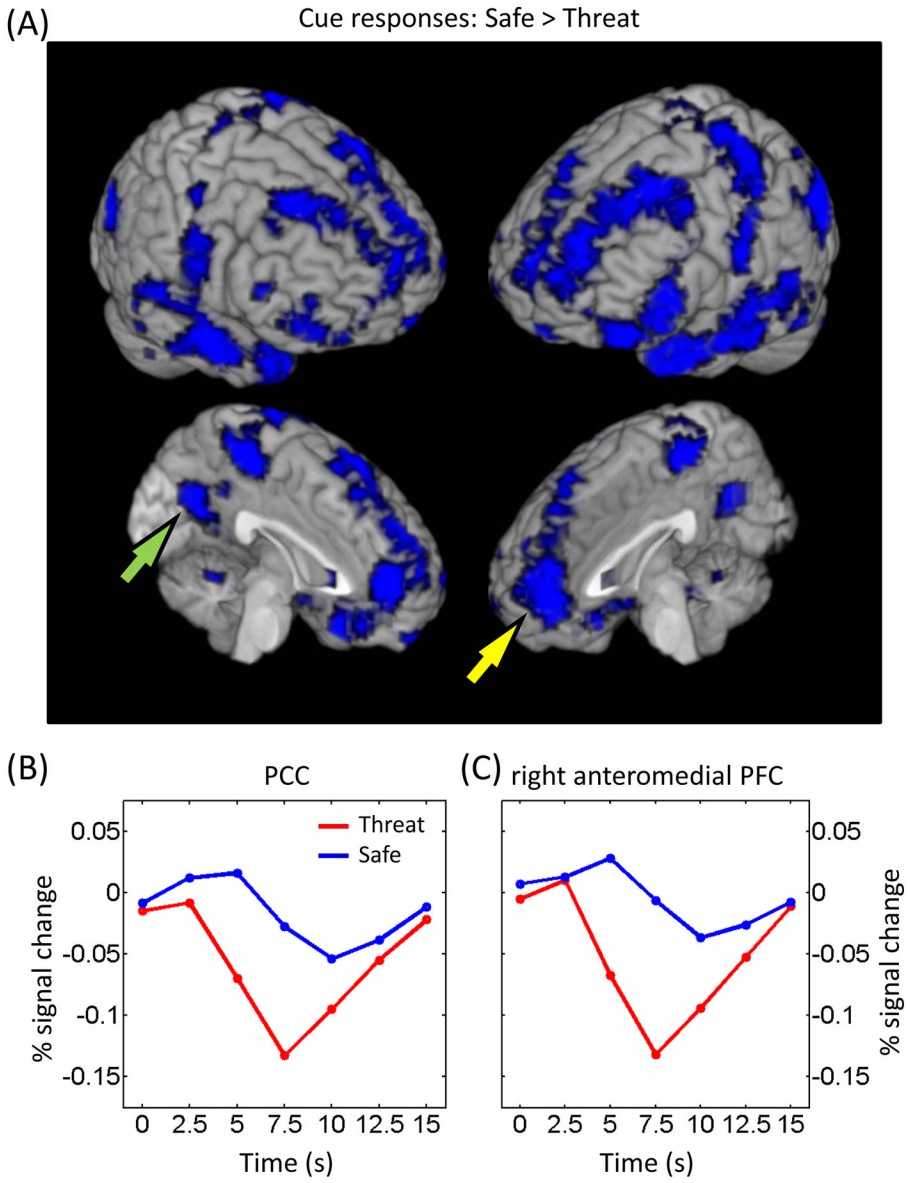

Figure 5.

Cue-related responses. (A) Voxels that showed stronger responses during safe than threat trials (displayed at $p < 0.05$, cluster-level corrected). The overall pattern was very similar to the one reported for the task-negative network. (B, C) Mean estimated responses from the PCC (B; see green arrow in panel A) and right anteromedial PFC (C; see yellow arrow in panel A) during safe and threat conditions. PCC, posterior cingulate cortex; PFC, prefrontal cortex.

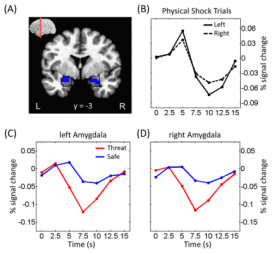

Figure 6.

Cue-related responses in the amygdala. (A) Voxels within the anatomically defined amygdala (as defined via the AFNI anatomical template; black outline) exhibiting stronger responses during safe vs. threat. (B) Mean estimated responses from the left and right amygdala during trials in which electrical stimulation was administered. (C, D) Mean estimated responses from the left (C) and right (D) amygdala during safe and threat conditions (as in all other analyses reported in the paper [except those of panel B], trials containing shock were discarded).

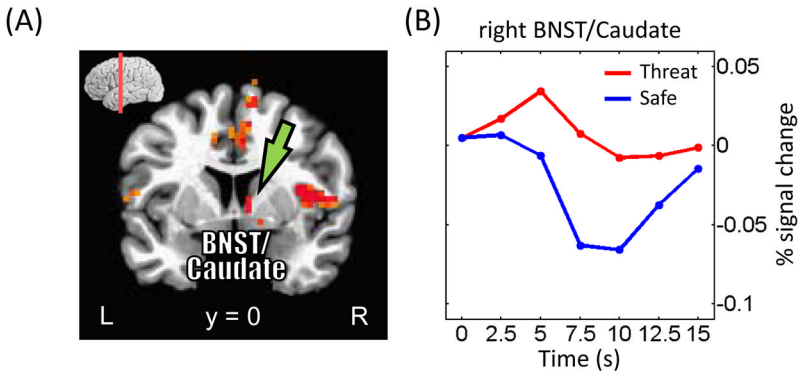

Figure 7.

Cue-related responses in the bed nucleus of the stria terminalus (BNST)/caudate. (A) Voxels that showed stronger responses during threat than safe trials (displayed at $p < 0.05$, cluster-level corrected). (B) Mean estimated responses from the right BNST/caudate (see green arrows in panel A) during safe and threat conditions. At an exploratory threshold of .001 (uncorrected), we observed similar responses in the left BNST/caudate.

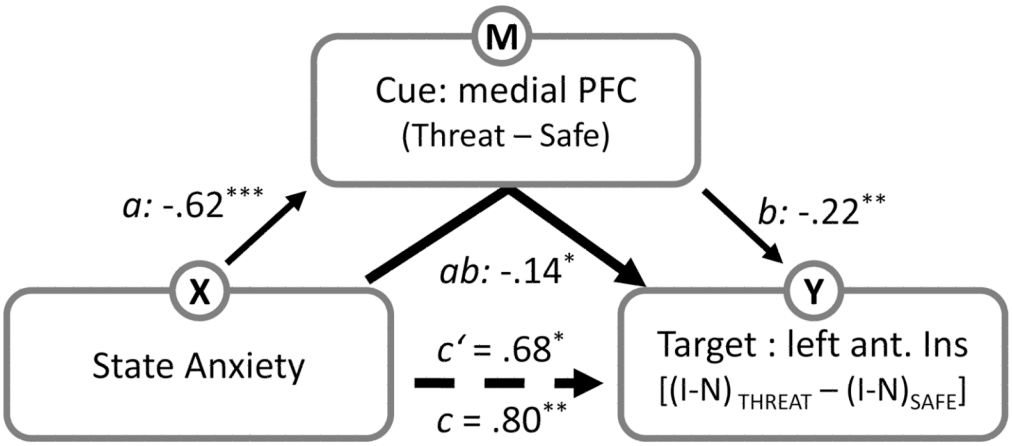

Figure 8.

Mediation analysis. We tested whether the relationship between state anxiety and target responses was mediated via responses at the cue phase. For the target phase, interaction-type scores were considered, whereas differential responses were considered during the cue phase. The letters a, b, c and c' refer to estimated path coefficients. The dotted line indicates the path coefficient was reduced after the mediator was taken into account. Ant. Ins; anterior insula. I, incongruent trials; N, neutral trials. *$p < .05$, **$p < .01$, ***$p < .005$.

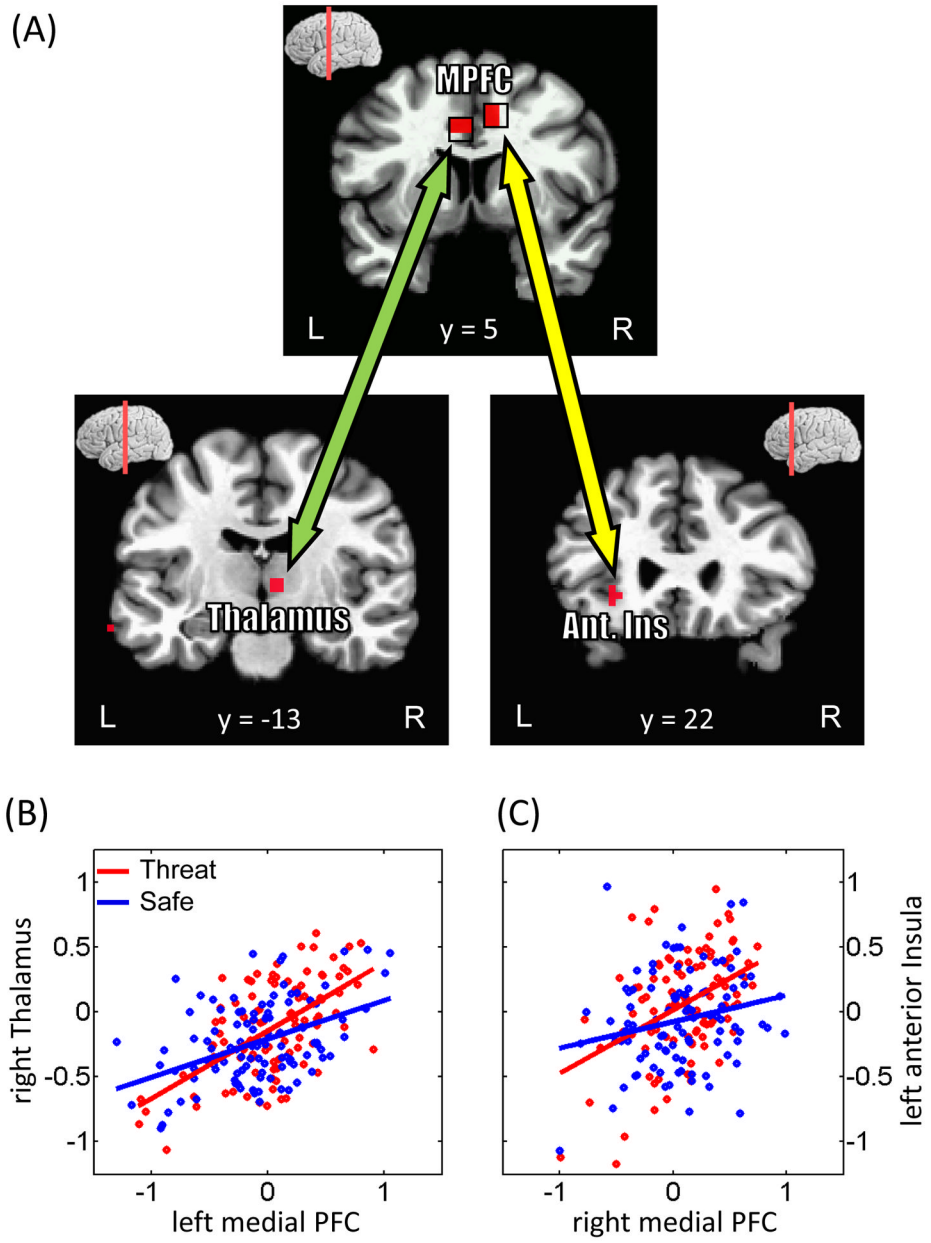

Figure 9.

Functional connectivity on a trial-by-trial basis. (A) Regions exhibiting stronger functional connectivity with the medial PFC during the cue phase. The top panel illustrates the ROIs employed as “seed” regions. MPFC, medial prefrontal cortex; Ant. Ins, anterior insula. (B, C) The scatter plots show trial-by-trial responses in the left medial PFC and right thalamus (B) and in the right medial PFC and left anterior insula (C). Responses to threat trials are shown in red and to safe trials are shown in blue. Robust linear fits to the data are presented in the corresponding colors. Data are illustrated for representative individuals.

Table 1

Voxelwise analysis at target phase (peak Talairach coordinates and *F* values)

Location		x	y	z	$F_{1,40}$
Incongruent > Neutral					
Temporal					
Fuisiform gyrus	L	−40	−55	−10	40.58
	L	−34	−37	−16	33.57
Parietal					
Precuneus	R	8	−70	38	18.36
Intraparietal sulcus	L	−31	−49	35	48.67
	R	29	−61	35	25.37
Frontal					
Frontal Eye Field	L	−34	−10	59	28.04
	R	29	−7	47	30.93
Supplementary Motor area	L/R	−7	2	50	80.94
Middle/Inferior Frontal gyrus	L	−37	17	23	71.49
	R	38	2	29	20.97
Anterior Insula	L	−28	17	8	29.99
	R	41	14	2	37.81
Medial Prefrontal cortex	L	−10	20	29	22.93
Cerebellum	L	−34	−61	−49	25.55
	R	8	−67	−28	24.47
	R	38	−58	−28	20.34

Table 2

Voxelwise analysis at cue phase (peak Talairach coordinates and *t* values)

Peak Location		x	y	z	t_{40}
Threat > Safe					
Parietal/Temporal					
Inferior Parietal gyrus/Superior Temporal gyrus	L	−58	−25	23	4.64
	R	62	−37	23	4.56
Frontal					
Posterior Inferior Frontal gyrus	L	−58	5	11	4.65
Posterior Inferior Frontal gyrus/Mid-insula	R	50	−1	8	5.34
Supplementary Motor area	R	8	2	56	4.59
Mid-insula	R	32	5	11	5.1
Medial Prefrontal cortex	L	−4	5	32	5.04
	R	11	5	38	4.87
Anterior Insula	L	−31	17	11	7.82
	R	29	20	11	8.58
Subcortical					
Thalamus	R	8	−13	8	6.47
BNST/Caudate	R	8	5	2	7.61
Basal Forebrain	R	14	−1	−4	4.00
Safe > Threat					
Temporal					
Inferior Temporal gyrus	L	−52	−46	−7	−4.9
	R	44	−61	−4	−4.46
Parahippocampal gyrus	L	−22	−40	−7	−5.12
	R	29	−43	−4	−4.75
Superior Temporal gyrus	L	−58	−13	2	−5.99
	R	59	−28	5	−5.72
Middle Temporal gyrus	L	−58	−10	−16	−5.31
	R	56	8	−19	−5.78
Superior Temporal gyrus/Temporal pole	L	−49	17	−13	−5.85

Peak Location		x	y	z	t_{40}
Inferior Temporal gyrus/Temporal pole	R	35	20	−31	−5.62
Parietal					
Angular gyrus	L	−46	−73	23	−6.13
	R	41	−61	23	−5.1
Posterior Cingulate cortex (Precuneus)		2	−58	26	−4.9
Postcentral gyrus	L	−31	−34	62	−5.59
	R	11	−34	62	−5.7
Paracentral lobule		5	−31	56	−6.42
Frontal					
Posterior Insula	L	−37	−16	17	−5.31
Precentral/Postcentral gyrus	L	−43	−13	29	−6.79
	R	59	−10	20	−6.91
Middle/Inferior Frontal gyrus	L	−37	8	29	−4.4
Superior/Middle Frontal gyrus	L	−25	11	50	−6.71
	R	23	23	50	−5.29
Superior Frontal gyrus	L	−19	53	26	−6.67
	R	8	59	14	−5.06
Ventromedial Prefrontal cortex (Rectal gyrus)		−4	23	−19	−4.99
Ventromedial Prefrontal cortex (Rectal gyrus)	L	−7	38	−7	−4.38
Inferior Frontal gyrus	L	−37	44	−7	−5.53
	R	47	41	5	−5.34
	R	29	35	−7	−5.08
Rostral Anterior Cingulate cortex	L	−7	44	11	−4.01
	R	8	44	2	−5.04
Subcortical					
Hippocampus/Amygdala	L	−19	−10	−13	−5.89
Hippocampus	R	23	−13	−13	−6.11
Amygdala	L	−21	−4	−12	−4.88
	R	17	−4	−12	−4.96
Cerebellum	R	23	−76	−34	−4.09
	R	38	−64	−34	−4.11

Table 3

Mediation analysis

Initial variable (X): state anxiety scores; Outcome variable (Y): target-related responses in the left anterior insula ROI

	Regression Coefficients (*p*-values)				
Mediator	**a**	**b**	**c′**	**c**	**ab**
medial PFC	−.62 (.004)	−0.22 (.006)	0.68 (.040)	0.80 (.009)	0.14 (.028)
right thalamus	−.80 (.005)	.01 (.777)	.80 (.040)	.80 (.009)	−.01 (.882)